Conf-920311--15

ANL/CP--74780

DE92 015185

SUMMARY OF RESULTS FROM THE TEXTOR HELIUM SELF-PUMPING EXPERIMENT

by

J.N. Brooks and A. Krauss
Argonne National Laboratory
Fusion Power Program
Argonne, IL 60439 USA

R.E. Nygren and B.L. Doyle
Sandia National Laboratories
Albuquerque, New Mexico 87185 USA

K.H. Dippel and K.H. Finken
IPP, Forschungszentrum Julich
Association Euratom-KFA
Julich, Germany

March 1992

* Work supported by the Office of Fusion Energy, U.S. Department of Energy under Contract Number W-31-109-Eng-38.

To be presented at the 10th International Conference on Plasma Surface Interactions in Controlled Fusion Devices, March 30 - April 3, 1992, in Monterey, California.

SUMMARY OF RESULTS FROM THE TEXTOR HELIUM SELF-PUMPING EXPERIMENT

J.N. Brooks and A. Krauss
Argonne National Laboratory
Argonne, IL 60439 USA

R.E. Nygren and B.L. Doyle
Sandia National Laboratories
Albuquerque, New Mexico USA

K.H. Dippel and K.H. Finken
IPP, Forschungszentrum Julich
Association Euratom-KFA
Julich, Germany

Abstract

Helium removal experiments were conducted in TEXTOR with a small helium self-pumping module located in a modified ALT-I limiter head. The module contained two heated nickel alloy trapping plates, a nickel deposition filament array, a Langmuir probe, flux probe, and thermocouples. The experiment examined plasma helium removal via trapping of helium ions in the deposited nickel surfaces. Such helium removal was successfully observed, with about 10% of the helium in a 10% He/D plasma being removed in a ~1 s period. The module was found to be compatible with overall tokamak operation with essentially no sputtered nickel entering the core plasma. The temperature rise on the ion-exposed inner trapping plate, during a plasma shot, is consistent with a local sheath potential of ~3 kT_e. Post-tokamak test examination of the trapping plates shows helium atom concentrations in the deposited nickel consistent with the observed helium removal, and shows very small D concentrations.

1. Introduction

The helium self-pumping concept [1] for fusion reactors is to remove helium in-situ by trapping impinging helium ions in freshly deposited metal layers of a limiter or divertor. A key requirement is for the deposited material to trap helium much better than hydrogen. Metals believed capable of preferential trapping include nickel, iron, vanadium, niobium, and molybdenum. The selective trapping in these metals is the result of the negligible solubility of helium in the lattice. Hydrogen, on the other hand, remains in solid solution (at suitably elevated material temperatures) until it escapes from the surface. By selectively trapping He and recycling DT, self-pumping potentially eliminates the need for vacuum pumping during the plasma burn, with consequent savings in cost and complexity, particularly in regards to neutron shielding of vacuum ducts and to processing of tritium.

Following encouraging laboratory tests of helium trapping in deposited nickel [2], a tokamak test module was built for TEXTOR and installed in November 1991. Due to several factors including a design-constrained reduction in trapping plate size, the module had less helium removal capability than originally estimated [2]. To observe helium removal by the module against a background removal by other processes in TEXTOR it was necessary to obtain very reproducible plasma conditions - this was accomplished over the course of a five shot-day experimental period.

In addition to the helium trapping results, the experiment provided an opportunity to examine sputtered impurity (nickel) transport as well as heat flow and sheath potential characteristics at an oblique-incidence magnetic field tokamak boundary surface - the inner trapping plate. The overall results are summarized in this paper with more detailed analysis to be reported in subsequent articles.

2. Self-pumping module

The basic module and experimental design is described in Ref. 2. The helium trapping module was installed inside the woven graphite ALT-I limiter head, and the entire assembly was mounted on the ALT-I support structure. The design is shown schematically in Fig. 1 and the ALT-I installed module is shown in Fig. 2. Plasma ions entering the ALT-I throat impinge on an inboard ~20 cm x 20 cm x .3 cm Inconel trapping plate, that can be coated with nickel between plasma shots. This plate is toroidally flat and curved poloidally along the minor radius in order to spread the heat flux in an approximately uniform manner. The plate intercepts the (total) magnetic field at highly oblique angles varying from 2.4° at the leading edge to 7.5° at the back. A second outboard trapping plate, of similar dimensions but flat, is not in the line of sight of incoming ions but can intercept and trap reflected particles.

Both plates have embedded thermo-coax heaters and thermocouples on their exterior. The outboard plate has a slot approximately 1/2" x 6" to permit viewing of six of the eight nickel deposition filaments. (This slot as well as other openings provide a conductance path for particles to enter the ALT-I holding fixture volume thereby providing a form of pseudo-pumping, to be discussed). Two thermocouples on each plate were used for control of the plate temperature, prior to a plasma shot, via input through a controller to a 4000 W plate heater supply. The heaters were turned off just prior to a plasma shot, in order to avoid generating magnetic fields.

The nickel deposition filaments consist of three twisted strands of 1.0 mm diameter W-3% Re wire, wrapped with three strands of 0.5 mm diameter pure nickel wire. The difference between the nickel melting point (1453°C) and the temperature at which significant nickel evaporation occurs is only 100-150°C, and it is therefore necessary to provide a mechanical support for the nickel

wire. In this design, the W-3% Re wire also functions as the heating element. W-3% Re was chosen because it was found to be much more resistant than pure W or Ta to embrittlement resulting from nickel alloying in case a partial melting of the nickel should occur. The filaments were arranged in two banks of four each. One bank was used as the active set, while the other bank was held as a spare in the event of a failure of the first set.

In order to prevent excessive thermal ramping of the filaments during deposition, the nickel deposition sequence consisted of two 7 minute deposition periods at 277 amps current (at ~3.3 volts) with a 2 minute cooldown period between. A two-color infrared pyrometer was mounted outside a window in the ALT-I housing so that it could view the filaments through the slot in the outboard plate. The measured filament temperature during deposition was typically in the range 1300-1350°C. Previous laboratory experiments found that one set of filaments could be expected to deposit approximately 50 Å of nickel on the trapping plates, per deposition sequence.

3. Operational conditions

TEXTOR is a medium size tokamak of major radius R = 1.75 m and a minor radius of a = 46 cm [3]. For the helium self-pumping experiments a plasma current of 350 kA, a toroidal magnetic field of B_T = 2.25 T, and a discharge length of ~3 s were used. Several plasma operational scenarios were implemented during the experimental period. One desired condition was to maximize the energy of impinging helium particles on the trapping plates. This was achieved by operating at low plasma densities, $\bar{N}_e = 1 \times 10^{19}\ m^{-3}$, and with neutral beam heating. The plasma electron density was kept at or above a level set by a deuterium injection feedback system and rose above this level when He was injected. Plasma electron temperatures of $T_e \approx 25$-35 eV and

density $N_e \approx 3 \times 10^{18}$ m^{-3} were measured at the ALT-I throat, under these conditions.

A second requirement was to avoid covering the nickel plates with deposited carbon (arising primarily from sputtering of the ALT-I front face) and also possibly saturating the plates with deuterium before the helium was even injected. To accomplish this, the discharge was started at the inner wall of TEXTOR and kept there until t = 1.2 s. Before the shift to the normal plasma position a short puff of helium was injected, at t = 0.8 s, leading to a helium concentration in the plasma of about 10%. The neutral beam was turned on during the interval 1.0 s $\leq$ t $\leq$ 2.7 s. The time intervals between the different steps are sufficient for a complete helium mixing and for establishing a steady state condition before the plasma can reach the entrance of the ALT-I limiter at t = 1.2 s. This technique, however, limited the effective pumping time of the module to about 1.5 s.

An additional issue is the competing effect of helium pumping by the TEXTOR first wall (surface area ~36 m^2) which can be fairly high [4]. To avoid a ratcheting of the helium wall concentration, at least two of the eight pumps of the toroidal pump limiter ALT-II were kept open at all times. This by-pass pumping had only a small effect on the removal during the discharge because ALT-I was positioned at a = 42.5 cm and ALT-II at 47.5 cm. This difference insures that the magnetic flux surfaces leading into the ALT-I throat are not blocked by any other limiter.

The helium removal experiments were then performed in the following way. After the ALT-I head was inserted into its final position (at a = 42.5 cm) a series of discharges (typically 5) were performed until the plasma conditions were stable from one shot to the next. Nickel deposition was then performed between plasma shots. During deposition, the ALT-I throat entrance

was closed by a shutter to avoid nickel contamination outside the module. The deposition lasted about 20 minutes. Following the nickel deposition a series of discharges were run and the helium removal was compared to shots without fresh Ni deposition.

4. Helium removal results

The plasma helium concentration was primarily assessed by spectroscopically monitoring the 468.6 nm HeII emission line at the tokamak boundary [4]. Figure 3 shows the measured helium content for a series of shots before, just after a nickel deposition, and a subsequent shot. The data shown have been time averaged to reduce high fluctuation rates in the raw data. The pre-shot plate temperature for this series was 450°C. The large jumps in the He signal in Fig. 3 are due to shifts in the measured levels when the beam is turned on and when the plasma is shifted. Shots 48859 and 48860 (prior to Ni deposition) 48861 (just after) and 48862 are shown. Shots 48859 and 48860 were taken 6 minutes apart and are very similar, indicating excellent shot-shot reproducibility. Most of the reduction in He during a shot was determined (by conducting a shot with the ALT-I throat closed) to be due to "virtual pumping" associated with gas flowing into the large plenum volume of the ALT-I holding fixture. The pumping associated with trapping in the nickel film can be found by comparing the rate of He decrease with a fresh Ni film to the rate of decrease with no deposition. A high resolution analysis of the data of the Fig. 3 shows that about 10% of the initial plasma helium content is removed by the module by the end of the discharge. This corresponds to a total of ~8 x 10^{17} He atoms removed by the module, during the discharge. A relatively high fraction (~50%) of the helium removed by the module occurs rapidly, $\lesssim$ 100 ms, with slower but steady trapping occurring thereafter.

Since shot 48861 occurred 23 minutes after shot 48860, it represented a different thermal history between shots, as a result of the nickel deposition sequence. In order to rule out both time and temperature-dependent effects as the cause of the reduced He level in shot 48861 we performed several "pseudo-deposition" shots which duplicated the nickel deposition sequence except that the filament current was reduced from the 277A value used for reference Ni deposition. As with other shots, the plate temperatures were regulated during the filament heating and a stable temperature was maintained at the 450° setpoint. It was found that the He level associated with shot 48866 (230A) (sufficient for a similar degree of heating but with no Ni deposition) shows a He level consistent with the pre-deposition shot 48860 to within the shot-shot reproducibility. Results from shot 48866 and other sequences of test shots appear, therefore, to rule out time and most if not all temperature dependent effects. Other Ni deposition shots, run with otherwise reproducible plasma conditions, show essentially the same helium removal behavior as Fig. 3.

Due to the limited machine time available, it was not possible to adequately assess helium removal as a function of parameters such as plate temperature. There is an indication, however, based on one shot, that a plate temperature of 210°C results in little or no helium trapping - a possible result of hydrogen competition for available traps, at this relatively low temperature.

Because of the way the plasma was maintained, with an average electron density kept approximately constant via deuterium injection, we did not assess the in-situ removal of deuterium, if any, by the module. Post-tokamak test examination of the trapping plates, however, discussed later, shows very little trapped deuterium. This is consistent with expectations of selective helium trapping of helium in the nickel.

5. Nickel and carbon contamination

To within experimental resolution, no additional nickel was found in the plasma after Ni deposition in the module. (A rather constant level of Ni originating from the Inconel liner is always observed). After the insertion of the ALT-I head a consistent increase in carbon level in the machine was seen. This additional carbon is most likely generated at the ALT-I graphite head. An edge carbon level of ~3% C/D was estimated from spectroscopic measurements.

The non-increase in plasma nickel content is consistent with the hypothesis that any Ni sputtered from the trapping plates is primarily redeposited within the module, as would be expected from the geometry. Such redeposition is due in theory e.g., see Ref. 5, to the short Ni atom mean-free-paths for ionization (e.g., $\lambda \approx 0.5$ cm for a 5 eV sputtered Ni atom at $T_e = 35$ eV, $N_e = 3 \times 10^{18}$ m^{-3}), and to frictional forces with incoming plasma ions which would inhibit Ni ion flow out of the throat.

6. Plate heating

From the thermal history and data on flux and electron temperature from the probes at the ALT-I throat, we can extract information about the sheath potential at the inner trapping plate. This information is useful to confirm the anticipated acceleration potential for implanting the He^{++} ions as well as for verifying estimates of sheath potential at oblique incidence, divertor-like surfaces (a critical issue for future tokamaks such as ITER).

The 0.318 cm thick Inconel plate has sufficient heat capacity to prevent a large average temperature rise. An analysis of the transient heating of the plate gives the correlation between the temperature at the back of the plate,

to which the thermocouples are brazed, and the temperature of the trapping layer at the plasma-facing surface.

Except for non-adherent surface layers, the effect of thin deposited layers on the temperature rise can be neglected. For a total deposited thickness of about 2000Å and a thermal conductivity ≥ 1% that for either Ni or carbon, the temperature differential across the plate would be less than 1°C.

Before thermal saturation (which occurs here at 0.5 s), the rise in temperature at the surface where the heat flux is applied depends primarily upon the heat flux divided by the conductivity. After thermal saturation the temperature rise is linear. The temperature rise at the surface is given by the equation below [6], in which q_o is the heat flux (at x = a), α is thermal diffusivity, k is conductivity and a is the thickness:

$$T(x.t) = \frac{2\, q_o}{k} \sqrt{\alpha\, t} \left\{ \sum_{n=0}^{\infty} 2\ \text{ierfc}\ \frac{(2\ n+1)a-x}{\sqrt{\alpha\ t}} + \text{ierfc}\ \frac{(2\ n-1)\ a-x}{2\ \sqrt{\alpha\ t}} \right\} \qquad (1)$$

Calculated rises in surface temperature for a range of heat fluxes are shown in Figure 4. A steady heat flux lasting 2.7 s is used here to approximate the thermal history of a particular set of shots (49225-30) in which the neutral beams remained on for 1.0 s after the plasma was shifted to ALT-I, then the shot continued for another 1.7 s with a lower heat flux on ALT-I. Also shown are temperature at the back of the plate and the equilibrium temperature after the surface heat flux is removed, which correspond to the thermocouple readings during and after a shot. Since thermal saturation is rapid and the thermocouple readings correspond to the average plate temperature, the basic quantity of interest is simply the heat stored in the plate.

For shot 49225, the temperature rise recorded by the thermocouple was 12°C. With the approximation above, a heat flux of 6 W/cm^2 produces a rise of 12°C in the equilibrated temperature after the shot and a rise of 14°C at the plasma facing surface of during the shot. However, the shape of the power loading, as judged by the product of T_e and j^+ is better characterized as a power level of 150% $\bar{q}$ for 1s, when the beam is on, and then 75% $\bar{q}$ for 1.7 s. Based upon this characterization, the appropriate power level to the plate during the (beam-on) helium trapping is about 9 W/cm^2.

With ALT-I inserted to 42.5 cm and a particle scrapeoff length of 2.2 cm (based upon previous data collected with probes at three radial positions at the ALT-I throat [7]), the calculated distribution of particle flux on the plate rises from about 71% of the average value at the leading edge to about 79% at the location of the thermocouples (1.6 cm from the leading edge) to a broad peak with a value of 110% about 2/3 of the way back and is 100% at the trailing edge.

The local ion flux, j^+, into the sheath near the location of the thermocouple was estimated using data from shots 49225-30 and the equation below. (Data on T_e was not available for shots 48860-64 and the conditions for 49225-30 were similar):

$$j^+ = \left[\frac{\exp\,(-a/b+c/d)\;\Gamma_{\text{flux probe}}}{W\,(b-a)}\right]\Phi\;\text{sine}\;(\theta) \qquad (2)$$

$\Gamma_{\text{flux probe}}$ is the total flux to the flux probe which extends 3 cm (linearly) from the top to the bottom of the ALT-I throat. Φ (0.79) is the ratio of the local flux to the average flux over the plate and θ (2.8°) is the local angle

of inclination. In the exponential term, a (3.115 cm), b (4.844), c (3.255), and d (6.248) are respectively the radial extents into the scrapeoff layer of the tops and bottoms of the plate and the probe. Based upon an ion current to the flux probe of 1.1 - 1.2 A., the average ion current density on the probe over the flux lines that connect with the plate is about 3.5×10^{18} q^+/cm^2 and the local ion current density on the plate is 2.4×10^{17} $q^+/cm2$. (With 10% He^{++} and 3% C^{+++} in the edge carried at the same velocity as the D due to viscous forces, the flux of D on the probe would be 5.0×10^{18} D/cm^2.)

If we assume that the sheath potential is established by deuterium, the majority species, then we can calculate a sheath transmission factor from the ion flux, electron temperature and power deposition inferred from the measured temperature rise of the plate. A power deposition of 9 W/cm^2 divided by the product of the local ion current density onto the plate of 2.4×10^{17} q^+/cm^2 and the electron temperature of 23 eV, measured with a Langmuir Probe at the throat of ALT-I, gives a sheath heat transmission factor of about $\gamma = 10$. This value is similar to the value of 8.5 predicted by Chodura [8] for the case of highly oblique incidence, $T_i = T_e$ and no secondary electron emission. This value of γ corresponds [8] to a sheath potential of $e\phi \approx 3$ kT_e.

7. Analysis of Ni trapping plates

At the conclusion of the experiment in TEXTOR, the trapping plates were removed from ALT-I and samples were sheared from the plates. Care was taken to clean all foreign matter from the shears and protect the surfaces of the samples. One sample each from the inner and outer plates, both at locations about 3.5 cm from the leading edges of the plates were analyzed. (Further analyses will be performed but were not available for this publication.)

He and deuterium were the elements of primary interest. Carbon is known to be present in high levels in the edge plasma in TEXTOR and the role of carbon contamination of the trapping surface is discussed later. Tungsten was expected because of the deposition filaments. Three different analyses were performed on the samples. Rutherford Backscattering Spectroscopy (RBS) with 7 MeV He^+ ions was used for W, Ni, O and C+B (range of ~5 μm); Elastic Recoil Detection (ERD) with 16 MeV Si^{+3} was used for He (range of ~250 nm); and Nuclear Reaction Analysis (NRA) with 700 keV $^3He^+$ (range of ~1 μm) was used to detect deuterium. The data is summarized in Table 1.

The measured He is expressed as a lower limit due to the effect of surface roughness. The depth resolution of ERD on a smooth sample is about 30 nm. When the surface roughness exceeds this value (here it is around 2.5 μm), then the width of the peak broadens with a corresponding decrease in height. Here depth resolution of the helium content and even an absolute determination of the helium inventory were not possible. Si with a relatively low energy range was selected to expose as much of the He peak as possible. (Increasing energy to obtain greater range brings interference from the C+B peak.) The "back edge" of the He was overlayed by the H peak. He that may be obscured by the H peak is ignored here, thus the reported He is some portion of the total areal density and provides a reliable lower limit. The upper limit, equal to the measured concentration times the roughness divided by the range, is about an order of magnitude larger.

The areal density of He of about $>2 \times 10^{16}$ He/cm^2 is consistent with expectations. Fresh Ni surfaces were deposited 21 times during the experiment in TEXTOR and the maximum expected trapping (in a pure Ni surface) at an implantation energy of around 100 eV would have been about 8×10^{16} He/cm^2 (21 times the measured [2,9] saturation value of 4×10^{15} He/cm^2). However,

carbon in the deposited layer may affect this result. A detailed discussion of helium implantation laboratory tests on TEXTOR - like evaporated Ni surfaces, and implications for tokamak trapping performance is given in reference 9.

Discussions with Dr. Jorg Winter of KFA regarding carburization and boronization studies of nickel and other surfaces at KFA indicated that, with Ni well above room temperature, deep penetration (~1 μm) of carbon into the lattice rather than a buildup could be expected. Thus, in the analysis here, the large amount of carbon observed may be distributed through the deposited Ni and even into the substrate rather than retained as discrete carbon rich layers over the deposited Ni layers.

To gauge the effect of carbon on He trapping, He implantations were done on a carbon contaminated sample. Ni samples were exposed for three hours at 350°C to a 90% hydrogen and 10% methane plasma in a discharge chamber at KFA. He implantations at 175 eV and subsequent analyses were done at Sandia. The saturation value of He in these samples was about 25% that of samples of as deposited Ni under similar conditions. If this reduced value of He saturation is applied to the trapping plates, then the anticipated He areal density in the plates would be about 2×10^{16} He/cm^2 which is the observed lower limit. This value is, in fact, equal to an areal density estimate based on the in-situ He removal data [21 SHOTS x 8×10^{17} He/SHOT/(2 x 400 cm^2)].

Further analyses of the plates and studies of samples may offer more insight into the effect of carbon on these results. The main point here is that the initial measurements of He trapped in the plates seems to be consistent with the observed levels of He self pumping in TEXTOR. Furthermore, the small quantity of D in the plates indicates that He was selectively trapped.

8. Conclusion

This experiment provided the first test of the self-pumping concept in a tokamak. While differing in several respects from a future fusion reactor embodiment of the concept, the TEXTOR test involved the following key elements: energetic helium ion impingement on a deposited nickel surface, the presence of much more (10x) hydrogen than helium, the presence of other contaminants, notably oxygen, and finally, a highly oblique trapping surface geometry with neutral particle reflection possible from one surface to another. A potentially serious complication was the presence of high carbon fluxes, originating from sputtering of the graphite limiter head. Fortunately, this did not prevent adequate nickel adhesion and subsequent helium trapping, though the carbon may have reduced the available trapping capacity.

As shown by both in-situ measurements as well as post-tokamak analysis of the trapping plates, the module was indeed able to remove helium from the plasma. The amount removed was modest in relation to the total helium content, but quite reasonable considering the limited trapping surface area. Very little deuterium was removed (possibly by the carbon), as evidenced by trapping plate analysis. This is an essential element of the concept in terms of recycling tritium back to the plasma, for future application. Little or no plate sputtered Ni reached the core plasma - a favorable result for both this concept and possibly for medium and high Z material surface applications e.g., for divertor plates.

Additional analysis of this experiment is planned, with other samples of the trapping plates to be examined in detail, and with additional assessment made of plate heating and other issues. Detailed trapping material tests such as effects on He trapping of temperature, H/He ratio, energies etc., are, for

practical reasons, probably best suited to laboratory testing and these are being planned. Possible follow up TEXTOR and/or other tokamak tests with, for example, a vanadium trapping surface are under consideration.

Acknowledgements

We would like to thank R. McGrath (SNLA), R. Mattas (ANL), and D. Smith (ANL) for critically helpful guidance and discussions during the course of this project, C. Outen (SNLA) and D. Walsh (SNLA) for help in the trapping plate analysis, and T. Banno (University of Tokyo), J. Boedo (UCLA), and D. Gray (UCLA) for their help at TEXTOR. Further thanks are due to J. Winter (KFA) and L. Grobush (KFA) for preparation of the carburized nickel samples and helpful discussions on the diffusion of carbon into nickel.

The U.S. portion of this work was supported by the U.S. Department of Energy, Office of Fusion Energy.

References

[1] J.N. Brooks and R.F. Mattas, J. Nuc. Mat. 121 (1984) 392.

[2] J.N. Brooks et al., J. Nuc. Mat. 176 & 177 (1990) 635.

[3] H. Soltwisch et al., Plasma Phys. Contr. Fusion 26 (1984) 23.

[4] K.H. Finken et al., J. Nuc. Mat. 176 & 177 (1990) 816.

[5] J.N. Brooks, Nucl. Tech./Fusion 4 (1983) 33.

[6] H. Carslaw and J. Jaeger, Conduction of Heat in Solids, Clarendon Press, Oxford (1959) 112.

[7] D. Goebel et al., Plasma Physics and Controlled Fusion 29 (1987) 473.

[8] R. Chodura in Physics of Plasma-Wall Interactions in Controlled Fusion, D. Post and R. Behrish ed. Plenum Press, NY (1986) pp.99.

[9] R.E. Nygren et al., J. Nuc. Mat. PSI-10, to be published.

Figure Captions

Fig. 1. Module design schematic and experimental geometry.

Fig. 2 Helium self-pumping module, installed in ALT-I limiter head (prior to tokamak installation). View is from back of outer trapping plate showing embedded heater elements and slot for viewing the nickel evaporation filaments and the trapping surface of the inner plate. The plasma enters module from the left through a 17 cm x ~3 cm shot (not shown) in the limiter head.

Fig. 3 Plasma helium content before and after nickel deposition.

Fig. 4. Calculated temperature rise on the inner plate as a function of surface heat flux.

Table Headings

Table 1. Analysis of Trapping Plates

Table 1. Analysis of Trapping Plates

Diagnostic	Element	Inner Plate Areal Density 10^{16} cm^{-2}	Outer Plate Areal Density 10^{16} cm^{-2}
ERD	He	1.9	1.6
NRA	D	0.3	0.3
RBS	NI	607 (89%)	479 (89%)
RBS	C+B	74 (9%)	63 (11%)
RBS	W	2	3
RBS	O	9	15

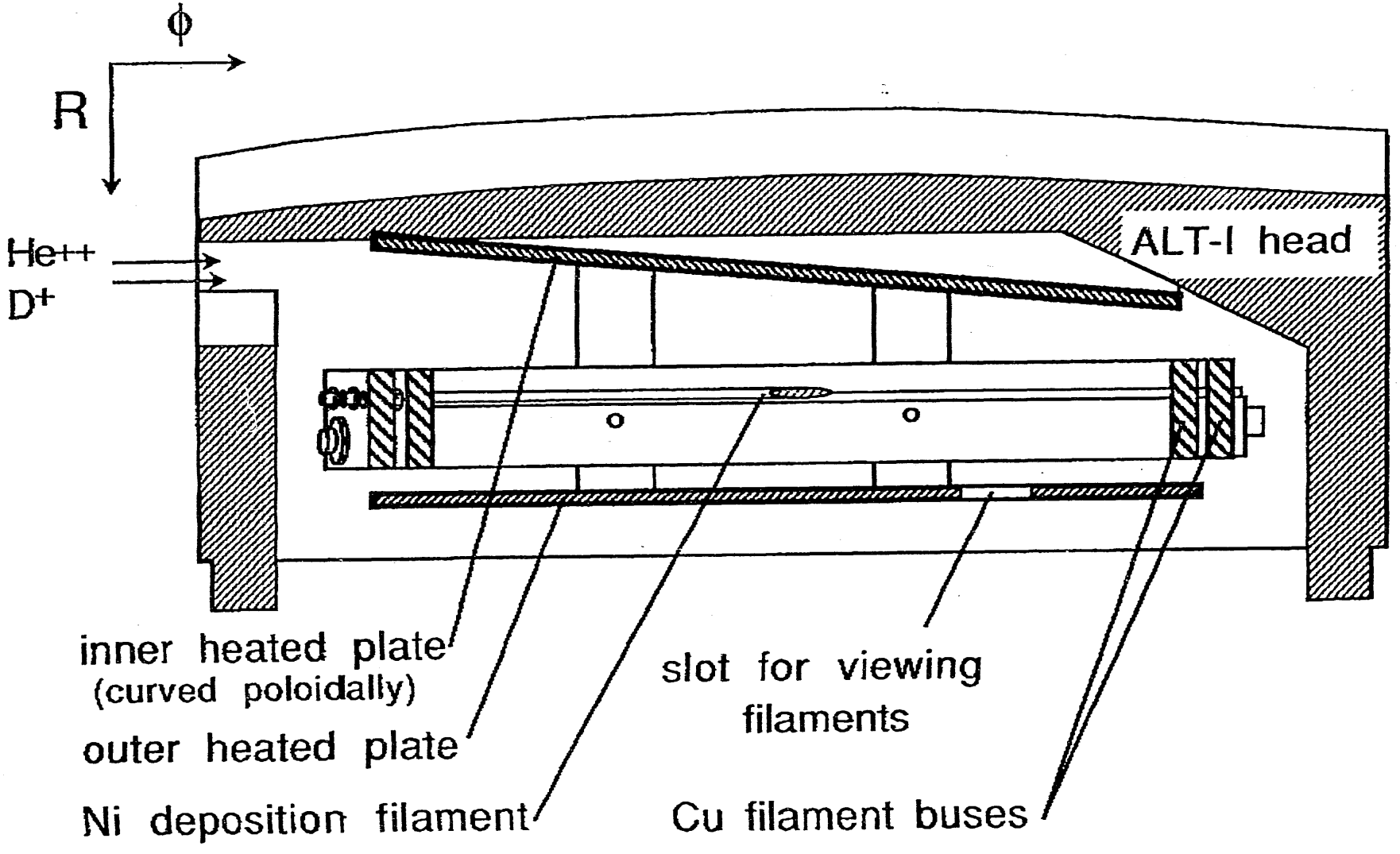
ϕ
R
He++
D+
ALT-I head
inner heated plate
(curved poloidally)
outer heated plate
Ni deposition filament
slot for viewing
filaments
Cu filament buses

FIGURE 1

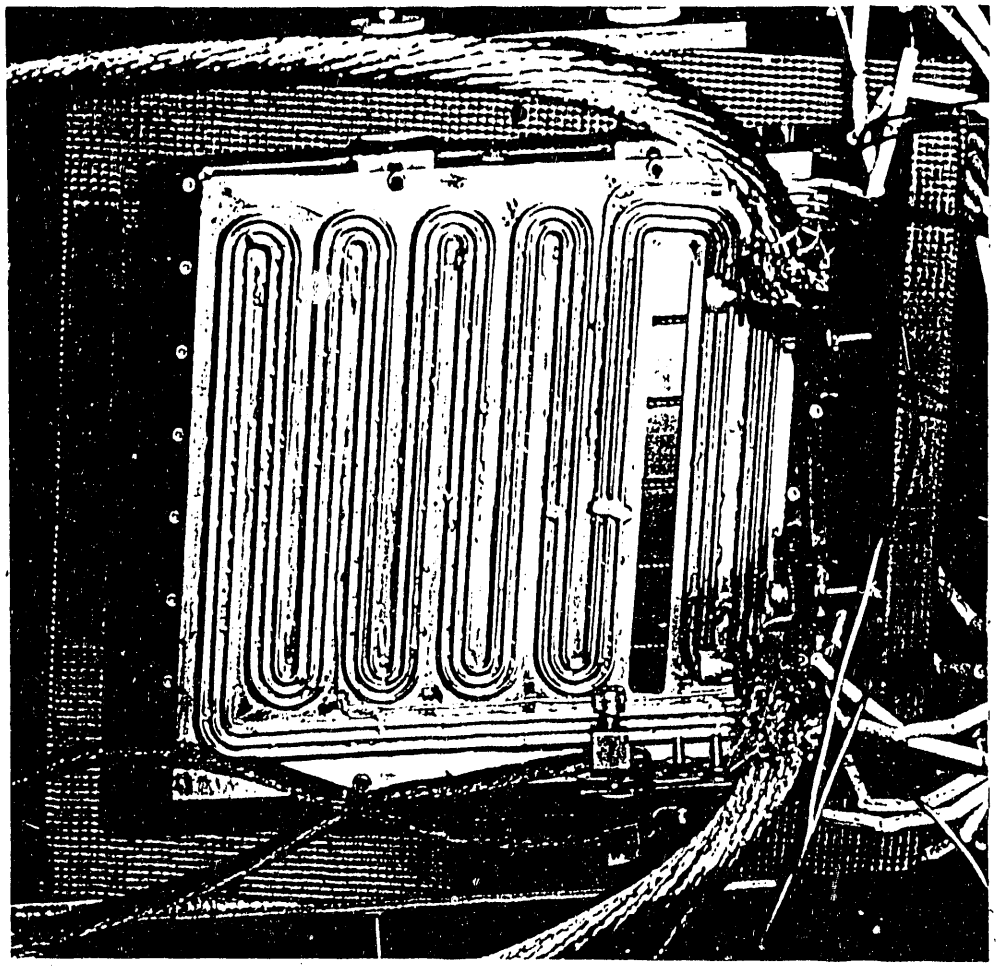

FIGURE 2

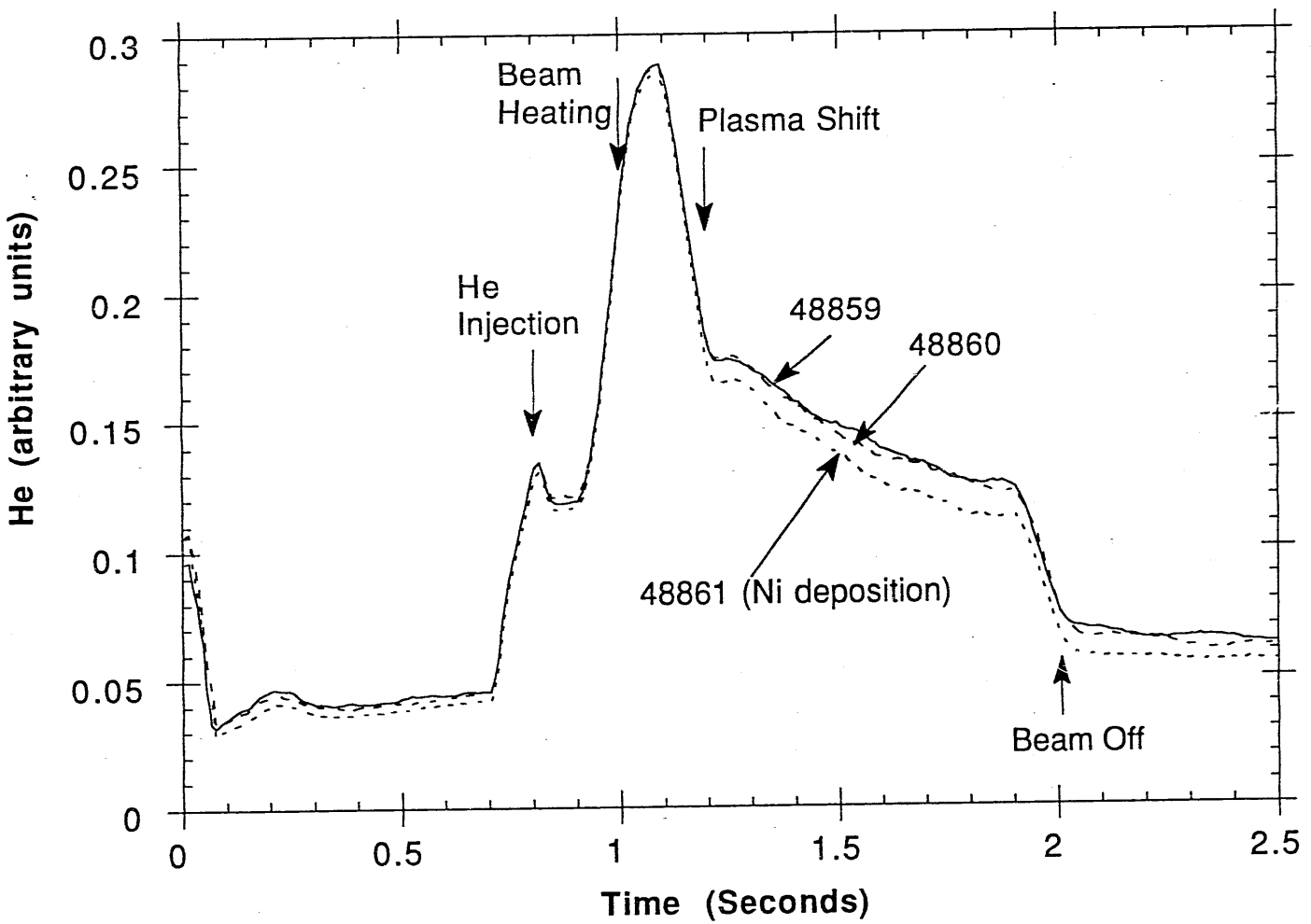
0.3
0.25
0.2
0.15
0.1
0.05
0
He (arbitrary units)
Beam
Heating
Plasma Shift
He
Injection
48859
48860
48861 (Ni deposition)
Beam Off
0
0.5
1
1.5
2
2.5
Time (Seconds)

FIGURE 3

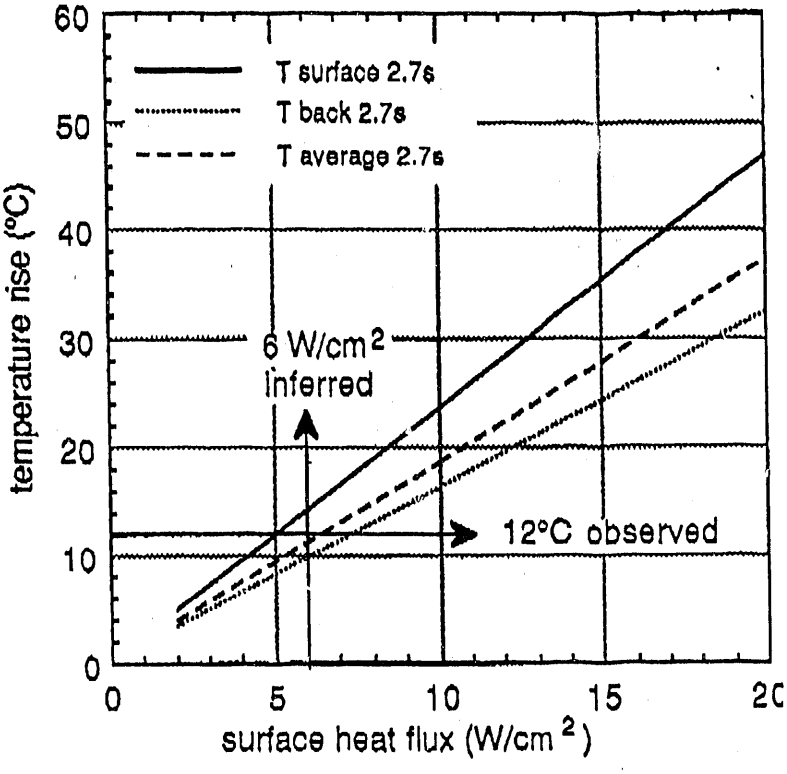
T surface 2.7s
T back 2.7s
T average 2.7s
6 W/cm2
inferred
12°C observed
temperature rise (°C)
surface heat flux (W/cm 2)
0
10
20
30
40
50
60
0
5
10
15
20

FIGURE 4

DATE
FILMED
7/22/92